# Spontaneous eyelid closures link vigilance fluctuation with fMRI dynamic connectivity states

Chenhao Wang[a], Ju Lynn Ong[a], Amiya Patanaik[a], Juan Zhou[a,b,1], and Michael W. L. Chee[a,1,2]

[a]Center for Cognitive Neuroscience, Neuroscience and Behavioral Disorders Program, Duke–National University of Singapore Medical School, National University of Singapore, 169857 Singapore; and [b]Clinical Imaging Research Centre, Agency for Science, Technology and Research (A*STAR), National University of Singapore, 117599 Singapore

Edited by Marcus E. Raichle, Washington University in St. Louis, St. Louis, MO, and approved July 8, 2016 (received for review December 7, 2015)

**Fluctuations in resting-state functional connectivity occur but their behavioral significance remains unclear, largely because correlating behavioral state with dynamic functional connectivity states (DCS) engages probes that disrupt the very behavioral state we seek to observe. Observing spontaneous eyelid closures following sleep deprivation permits nonintrusive arousal monitoring. During periods of low arousal dominated by eyelid closures, sliding-window correlation analysis uncovered a DCS associated with reduced within-network functional connectivity of default mode and dorsal/ventral attention networks, as well as reduced anticorrelation between these networks. Conversely, during periods when participants' eyelids were wide open, a second DCS was associated with less decoupling between the visual network and higher-order cognitive networks that included dorsal/ventral attention and default mode networks. In subcortical structures, eyelid closures were associated with increased connectivity between the striatum and thalamus with the ventral attention network, and greater anticorrelation with the dorsal attention network. When applied to task-based fMRI data, these two DCS predicted interindividual differences in frequency of behavioral lapsing and intraindividual temporal fluctuations in response speed. These findings with participants who underwent a night of total sleep deprivation were replicated in an independent dataset involving partially sleep-deprived participants. Fluctuations in functional connectivity thus appear to be clearly associated with changes in arousal.**

dynamic connectivity states | resting-state fMRI | vigilance | eyelid closure | sleep deprivation

The existence of large-scale functional brain networks is evidenced by well-defined spatial patterns of correlated blood-oxygenation level-dependent (BOLD) signal fluctuation in fMRI data (1). Recent work has shown that functional connectivity (FC) within and between brain networks is dynamic, corresponding to the observation that even while we are performing a task, our mental focus fluctuates (2). Fluctuation of fMRI-based FC occurs over tens of seconds (3, 4) and exhibits different patterns across conscious and unconscious states (5, 6). Furthermore, just as interindividual differences in stationary FC relate to variation in human behavior and cognition (7–10), it seems likely that recurring patterns (11) of fluctuating FC have behavioral significance.

Temporal fluctuations in FC can arise from conscious mental activity (12), episodes of random synchrony (3), or simply time-varying levels of physiological noise (13, 14). The association between BOLD signal fluctuation in the default mode network (DMN) and mind-wandering episodes (15–17) has prompted investigations into the behavioral correlates of spontaneous resting-state FC fluctuations (11, 18). Although these fluctuations in FC have been shown to correlate with several physiological markers, such as electroencephalogram (EEG) power, magnetoencephalography (MEG) power, and heart rate variability (19–21), their behavioral significance remains unclear.

A key obstacle to elucidating clear FC–behavioral state relationships is the difficulty in evaluating mental state without the use of an intrusive stimulus or behavioral probe. For example, in mind-wandering experiments, the experience sampling technique used to identify such epochs involves periodically probing (and interrupting) participants for meta-awareness of mental drifting (22).

To circumvent having to use probes to evaluate mental microstates, spontaneous eyelid closures (SEC) were used as a proxy for vigilance state. In sleep-deprived persons, the degree of SEC is an excellent marker of reduced responsiveness to auditory signals (23). Pronounced SEC, referring to epochs when the eyelids are closed or almost completely closed, correspond to periods when participants are less likely to respond to standardized auditory stimuli. SEC so robustly foreshadow behavioral lapses that they are commercially used for drowsiness detection (24, 25).

We recently found that time-locking FC estimation to the onset of pronounced SEC reveals accentuated forms of the stationary FC shifts observed in sleep-deprived healthy young adults compared with when they are well rested (26). These FC changes involve decreased within-DMN and within-dorsal attention network (DAN) connectivity, as well as reduced anticorrelation between DMN and DAN (27–30). In the present work, we sought to demonstrate that spontaneous FC fluctuations in sleep-deprived persons correspond to fluctuations in arousal that coincide with pronounced SEC. Motivating this approach are the twin observations that: (*i*) psychomotor vigilance in sleep-deprived persons shows pronounced moment-to-moment fluctuation (31), giving rise to sufficient state variance needed for

## Significance

**Functionally connected brain networks exhibit recurring connectivity fluctuations. Although such dynamic connectivity states (DCS) can be expected to have behavioral correlates, linking fluctuating connectivity with behavioral state is hampered by the use of mental probes that themselves perturb observed behavior. Using the degree of eyelid closure as a proxy for vigilance state, we were able to continuously assay behavior and constrain the myriad of possible DCS to two relevant states denoting arousal in sleep-deprived persons. Intriguingly, these two DCS had counterparts in task-based data that predicted interindividual differences in the frequency of behavioral lapsing and intraindividual fluctuations in response speed. The replication of these findings in an independent dataset should encourage further investigations into the network dynamics of mental states.**

Author contributions: C.W., J.Z., and M.W.L.C. designed research; C.W., J.L.O., J.Z., and M.W.L.C. performed research; C.W. contributed new reagents/analytic tools; C.W., J.L.O., J.Z., and M.W.L.C. analyzed data; and C.W., J.L.O., A.P., J.Z., and M.W.L.C. wrote the paper.

The authors declare no conflict of interest.

This article is a PNAS Direct Submission.

Freely available online through the PNAS open access option.

[1]J.Z. and M.W.L.C. contributed equally to this work.

[2]To whom correspondence should be addressed. Email: michael.chee@duke-nus.edu.sg.

This article contains supporting information online at www.pnas.org/lookup/suppl/doi:10.1073/pnas.1523980113/-/DCSupplemental.

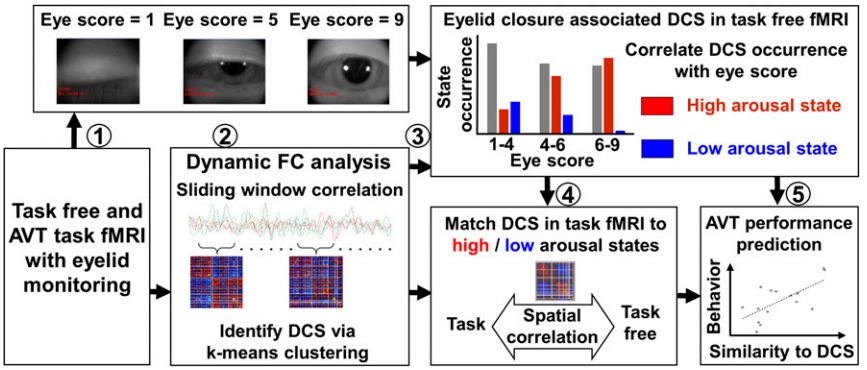


**Fig. 1.** Graphic overview of the study. (Step 1) Task-free and AVT fMRI scans were collected following total sleep deprivation. The degree of SEC was rated. (Step 2) DFC analysis was performed to extract DCS. (Step 3) DCS corresponding to a high- and low-arousal state associated with eyelid closure were derived. (Step 4) DCS derived from the AVT task fMRI dataset were matched to their counterpart templates in the task-free condition. (Step 5) High- and low-arousal DCS thus derived had intersubject and within-subject behavioral correlates.

reliable state classification; and (*ii*) prolonged SEC are more likely in the sleep-deprived state. We anticipated that spontaneous SEC in the sleep-deprived state would be associated with dynamic FC (DFC) changes in the DMN and DAN, incurring both within- and between-network shifts. We additionally expected that such dynamic connectivity patterns corresponding to "low-arousal" SEC epochs would coincide with behavioral lapses during an auditory vigilance task, and that this could be demonstrated within and across participants. We tested the reproducibility of our findings with an independent dataset involving partially sleep-deprived participants. Taken together, these predictions, if true, would support to the notion that specific patterns of DFC fluctuation correspond to variations in arousal level.

## Results

**Fluctuations in FC at Rest Are Associated with SEC in Sleep-Deprived Participants.** To elucidate the different time-varying patterns of whole-brain FC, we used a sliding-window approach to compute windowed covariance matrices from BOLD time courses extracted from the 126 predefined regions of interest (ROIs) in each participant (Fig. 1, step 1; details in *Materials and Methods*). Each was computed over a 40-s sliding window, shifted in 2-s increments (32). To estimate recurring DFC patterns, we performed *k*-means clustering on the aforesaid windowed covariance matrices pooled across all of the participants (Fig. 1, step 2). Each resulting cluster centroid was taken to be the exemplary FC pattern associated with each of several dynamic connectivity states (DCS) (Fig. S1, *Left*). Each frame in successive time windows was thus assigned with membership to one of these distinct DCS.

We next correlated the occurrence probability of each DCS with the SEC score (1, closed; 9, open) at corresponding time windows (Fig. 1, step 3). The occurrence probability of each DCS was based on the membership of each window as determined using *k*-means clustering at different degrees of SEC. We found two DCS that were either positively (Fig. 2, *Left*) (Spearman's $\rho = 0.905$, $P = 0.005$) or negatively (Fig. 2, *Right*) (Spearman's $\rho = -0.970$, $P < 0.001$) associated with SEC scores [$P < 0.05$ family-wise error rate (FWE) -corrected] (see Table S1 for the state distribution of these two DCS across subjects). No other DCS were associated with SEC. A random-effects group-level analysis showed that this SEC–DCS association was significant in most subjects ($P = 0.028$, $t = 2.20$; mean Spearman's $\rho = 0.372 \pm 0.535$ and $P < 0.001$, $t = -4.63$ and mean Spearman's $\rho = 0.461 \pm 0.373$ for positive and negative SEC–DCS correlations, respectively). This finding remained robust even with different numbers of clusters $k = 3$, 5, and 7 and with different sliding-window lengths (*SI Results* and Figs. S2 and S3). Additional analyses involving a high number of clusters ($k = 11$ and 13) showed largely the same results (*SI Results* and Fig. S4).

**High- and Low-Arousal States Exhibit Within-Network and Between-Network Differences in FC.** Having determined how different DCS relate to eyelid closure (SEC scores), we next characterized how FC patterns differed between high- and low-arousal DCS. To this end, we gathered a pair of windowed covariance matrices from each participant corresponding to the high- and low-arousal DCS. To minimize the effects of noise and clustering error, only windows corresponding to DCS identified as "high-" or "low-" arousal in more than 50% of the clustering results, and with different *k* values, were used. Averaged covariance matrices for high- and low-arousal DCS were thus obtained (Fig. 3, *Upper*, and *SI Materials and Methods*). Comparison between the two groups of matrices, using two-sample *t* tests on Fisher's *Z*-transformed Pearson correlation coefficients, revealed FC differences between these DCS ($P < 1E\text{-}6$ FWE-corrected) (Fig. 3, *Lower*).

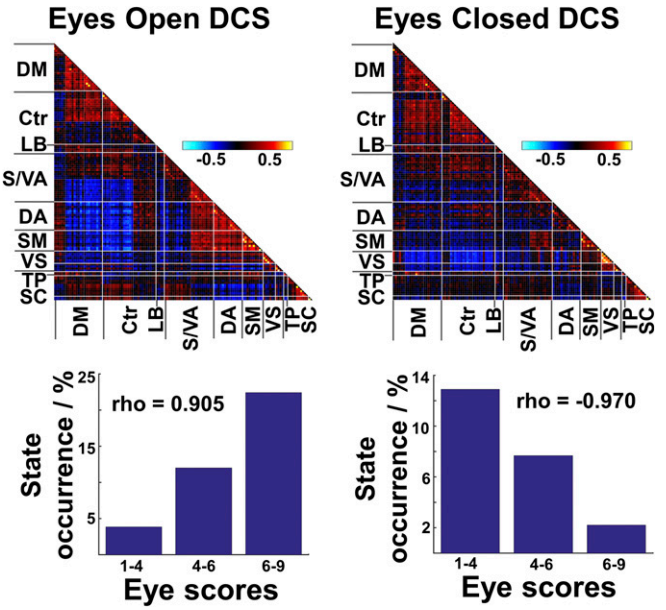


**Fig. 2.** DCS associated with predominantly eyes-open and eyes-closed states in the task-free condition. FC matrices of the two DCS associated with higher (eyelids open) and lower (eyelids closed) eye scores. For clearer illustration here, eye scores are binned into three levels. Spearman's ρ was computed with eye scores binned into eight levels (Fig. S8). Cool and hot colors denote negative and positive correlations respectively. Bars denote the frequency of occurrence of each DCS at different SEC ratings. Ctr, executive control network; DA, dorsal attention network; DM, default mode network; LB, limbic system; SC, subcortical regions; SM, somatosensory and motor network; S/VA, salience/ventral attention network; TP, temporal parietal network; VS, visual network.

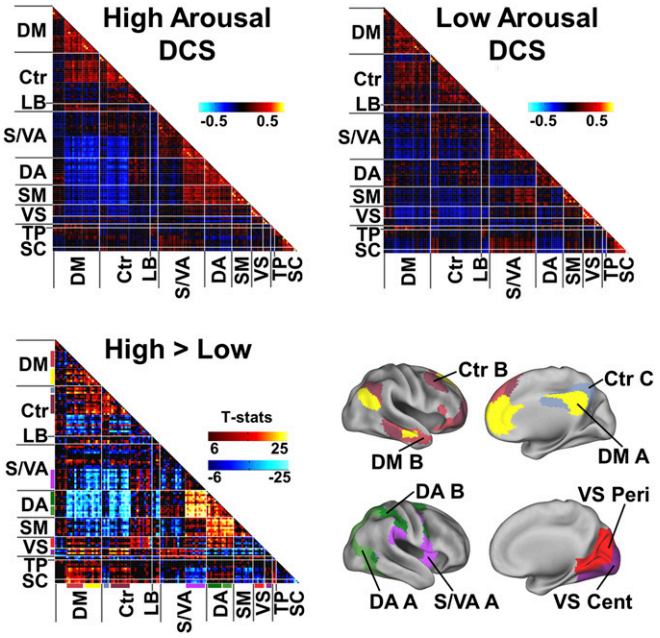


**Fig. 3.** Distinct patterns of within- and between-network FC in high- and low-arousal DCS in the task-free condition. (*Upper*) Averaged FC patterns associated with high- (*Left*) and low- (*Right*) arousal states. (*Lower*) Matrix of two-sample *t* test results related to FC differences between high- and low-arousal states, thresholded at $P < 1E\text{-}6$ few-corrected (*Left*). Networks showing significant FC differences across arousal state are color coded on the brain surface maps (*SI Materials and Methods*) (*Right*). Cent, central; Peri, peripheral; other abbreviations are as in Fig. 2.

Compared with the low-arousal DCS, the high-arousal DCS displayed higher within-network connectivity (Fig. 3, *Lower Left* matrix, diagonal cells) involving the DMN, control network, ventral attention/salience network (SN), and DAN. Higher between-network connectivity (Fig. 3, *Lower Left* matrix, off-diagonal cells) was also observed between the DMN and control network, between the SN and DAN, and between somatosensory networks and DAN. High arousal was accompanied by greater anticorrelation between the DMN (extending to control network) and DAN/SN. In contrast, the low-arousal DCS featured decoupling (lower correlation) between the visual network and higher-order cognitive networks, including the DMN, control, and DAN. Furthermore, in the low-arousal DCS, subcortical regions, specifically the thalamus and striatum, showed increased FC with SN and greater anticorrelation with DAN.

**DFC States Derived from Task-Based fMRI Resemble Those Derived from Task-Free fMRI.** To examine if DCS derived from task-free fMRI data could be mapped to low-arousal DCS derived during task performance, we ran the identical sliding-window analysis on data collected from the same participants as they performed an auditory vigilance task after total sleep deprivation (26). An additional step was taken to regress out task-related activation from BOLD time courses (Fig. 1, step 4). From the resulting FC cluster centroids (DCS derived from task-based fMRI data) (Fig. S1, *Right*), we found distinct DCSs that closely resembled the high- and low-arousal DCS derived from the task-free dataset. The resemblance between task-free and task-based DCS patterns was stronger in the high-arousal state. The low-arousal DCS matrices were spatially similar, particularly in on-diagonal elements. In the off-diagonal elements, differences between the states were clearer in the task-free data, and could represent an interaction between task performance and connectivity.

Importantly, high spatial similarity ($r > 0.85$) between the DCS was found regardless of the window length (Fig. S3) or the number of clusters used. We then used the same approach to summarize the clustering results across different $k$'s (as described above) to produce averaged windowed covariance matrices associated with high- and low-arousal DCS in the task condition (Fig. 4, *Left*). Similar within- and between-network FC differences were observed compared with the task-free analysis (Fig. S5).

**DCS Predict Interindividual Differences in Behavioral Performance.** We next investigated if arousal-associated DCS could predict interindividual differences in vigilance performance. To answer this question, we specified an individual's auditory vigilance task (AVT) performance using the proportion of behavioral lapses across all trials (60 min). An individual's lapse frequency was positively correlated with dwell time in the low-arousal DCS ($\rho = 0.465$, $P = 0.022$) and negatively correlated with her dwell time in the high-arousal DCS ($\rho = -0.584$, $P = 0.003$) (Fig. 4, *Right*). The third DCS, the one identified as neither low- nor high-arousal DCS, did not significantly correlate with an individual's AVT task performance ($r = 0.118$, $P = 0.583$). These findings were obtained using cluster number $k = 3$, but were also largely replicated using other $k$ values (values 5, 7, and 9) (*SI Results* and Fig. S6).

**Fluctuations in Dynamic Connectivity and Vigilance Are Linked.** In addition to predicting individual differences in vigilance across the entire experiment, we wondered whether fluctuations in FC patterns could inform us about intraindividual fluctuation in AVT response times. To quantify fluctuations in FC with respect to the identified high- and low-arousal DCS, we computed the spatial similarity of each windowed covariance matrix to these

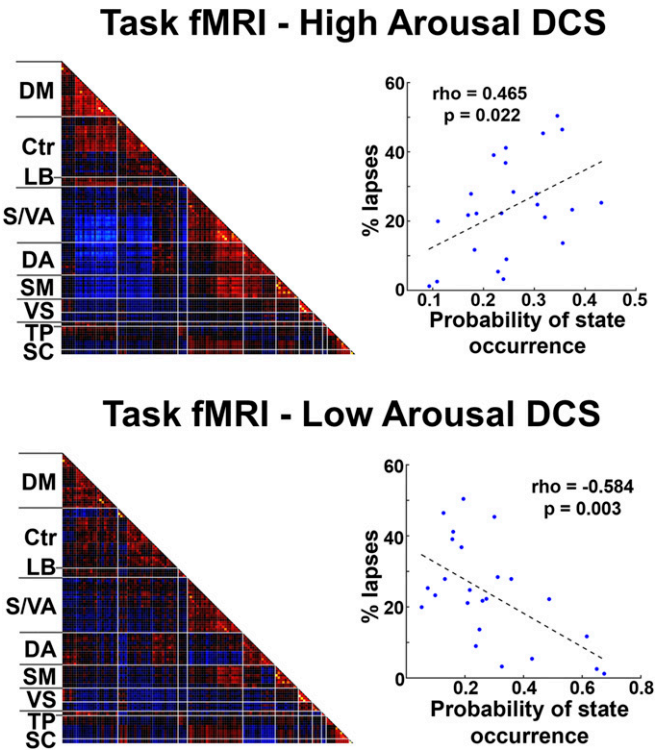


**Fig. 4.** Occurrence of high and low DCS correlated with individual differences in AVT task performance. (*Left*) The high- and low-arousal states derived from AVT task data exhibited similar patterns as those derived from task-free data (compare with Fig. 3). (*Right*) Participants with fewer instances of the high-arousal state and more occurrences of the low-arousal state had a higher proportion of lapses in relation to total trials. Abbreviations as in Fig. 2.

states using partial correlation. We used the rank-ordered mean reaction time of all trials within each successive sliding window to quantify temporal variation in arousal (*Materials and Methods*).

For each participant, faster responses corresponded to periods of greater spatial similarity to the FC pattern associated with high arousal. Conversely, when there was high spatial similarity to the FC pattern associated with low arousal, participants either responded more slowly or not at all (Fig. 5). Across participants, the correlation between the similarity of DCS expression to either high- or low-arousal state, and reaction time was $r = -0.325 \pm 0.208$ ($t = -7.60$, $P < 0.001$) for high-arousal state and $r = 0.298 \pm 0.187$ ($t = 7.72$, $P < 0.001$) for the low-arousal state. These findings remained significant after accounting for the number of stimuli presented in each time window and autocorrelation (*SI Results*). Moreover, the correlation between the similarity of DCS expression to the non-SEC–associated state and reaction time was not significant ($r = 0.047 \pm 0.146$, one-sample $t$ tests $P = 0.129$) (*SI Materials and Methods*).

**Replication of Key Findings Using an Independent Dataset Involving Partial Sleep Deprivation.** To test the robustness of our findings, we analyzed another independent dataset of partially sleep-deprived participants using the identical steps outlined for participants who underwent a single night of total sleep deprivation. Earlier findings were replicated at all levels of analyses, including the SEC–DCS association in the task-free data and the DCS–vigilance relationship associated with AVT task performance (both interindividual difference and intraindividual temporal fluctuations) (*SI Results*, *Replication Study*, and Fig. S7).

## Discussion

We studied time-varying whole-brain FC under task-free and task conditions in healthy young adults undergoing a single night of total sleep deprivation. Using degree of SEC as a proxy for level of arousal, we identified recurring FC patterns in the task-free data that conformed to high- and low-arousal DCS, respectively. These states showed systematic differences in FC. The high-arousal state was associated with greater intranetwork connectivity involving the DMN, control, and attention networks, as well as greater anticorrelation between the DMN and attention networks. Visual network, striatal, and thalamic connectivity also differed between the two states. The same two DCS could be identified after regressing out task-related signals associated with performing an AVT. Critically, we found that high- and low-arousal DCS could independently predict interindividual differences in frequency of behavioral lapsing as well as intraindividual fluctuation in response speed. Attesting to their robustness, these findings were replicated using an independent dataset involving partially sleep-deprived participants.

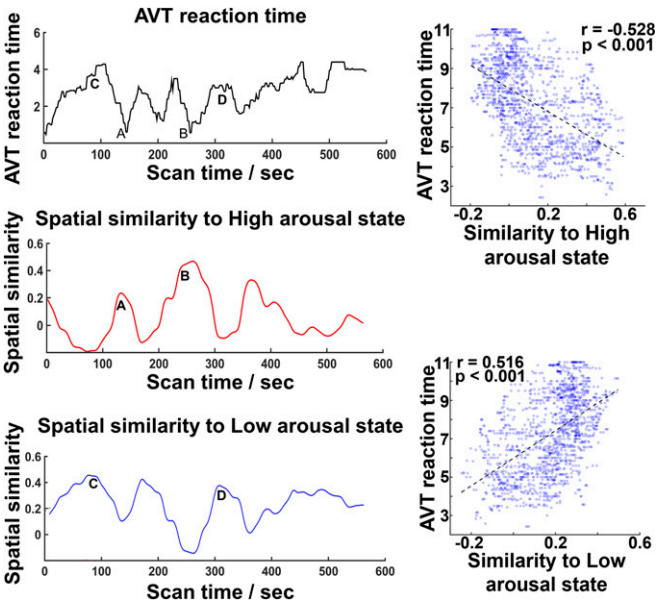


**Fig. 5.** Fluctuations in DCS correlated with response-time fluctuations. (*Left*) Time courses of AVT reaction time (*Top*), spatial similarity scores with the high-arousal DCS (*Middle*), and low-arousal DCS (*Bottom*) in a representative participant. "A" and "B" mark time points of fast AVT performance. Conversely, "C" and "D" mark time points of slow AVT performance. (*Right*) Time windows exhibiting high spatial similarity to the high-arousal DCS were associated with shorter reaction times. Time windows exhibiting high spatial similarity to the low DCS were associated with slower responses or lapses.

**Linking Fluctuations in FC and Behavioral State.** Brain activity during task-free fMRI experiments does not remain in a stationary resting state (33, 34). It has been established that spontaneous fluctuations in intrinsic FC are not simply noise (35) and can be correlated with physiological markers, such as EEG or MEG power at different frequency bands (19, 20), as well as with heart rate variability (21). Shifts in EEG power in the α- and θ-bands correspond to changes in arousal (36–38). Although these results are of physiological relevance, they only indirectly link FC fluctuation and behavioral state, require the use of technically demanding and expensive simultaneous EEG–fMRI methodology, and are difficult to deploy for real-time behavioral assessment. In contrast, monitoring eyelid closure is simple to implement and predicts an increased likelihood of behavioral lapses (23–25, 39). As such, SEC provides readily implementable measure to connect FC fluctuation with behavioral state.

We previously showed that prolonged SEC (distinct from blinks in awake persons) in the sleep-deprived state likely represent brief sleep intrusions (microsleeps) during which responses to auditory stimuli are slow or absent. Sensory threshold elevation during sleep (40) results from reduced transmission of sensory information to higher cortical areas. Specifically, higher cortical processing of sensory inputs, necessary for speedy responses to target stimuli, is attenuated as sleep deepens and higher cortical areas become progressively more isolated from brainstem, subcortical, or primary sensory cortical inputs (41).

Sleep deprivation (27–29) and falling asleep (42, 43) have both been associated with reduced FC within the DMN, as well as reduced anticorrelation between task-positive networks and the DMN. These alterations in FC have also been observed during periods of mind-wandering in the absence of meta-awareness (33) and during eyes-closed rest compared with eyes-opened rest (44). It has been proposed that "descent to sleep" is facilitated by both reduced thalamocortical connectivity at sleep onset (45) and a breakdown of general connectivity associated with deeper, slow-wave sleep (30). Both of these processes reduce the brain's capacity to integrate information across functional modules (30, 43, 46, 47). Anticorrelation between the DMN and task-positive networks in particular, is thought to reflect the competitive balance between internally and externally oriented cognition and is weakened in conditions of reduced consciousness (48, 49). Indeed, persons evidencing stronger anticorrelation between the DMN and attention networks in the well-rested state appear to be more resilient to sleep deprivation (29).

These observations notwithstanding, the relationship between FC and behavior remains enigmatic. For example, although on the average decline in the DMN and DAN FC with sleep deprivation is associated with increased lapsing, the extent to which stationary FC is altered does not correlate with the frequency of behavioral lapsing (28, 29).

The current strategy of selecting polar DFC states by constraining them with a continuously observable but proxy of behavioral state (SEC) allowed us to transcend the limitations of

using static FC of limited networks to uncover FC and behavior mappings. The utility of using SEC in the context of fMRI recordings was recently explored in two studies. The first study documented differences in resting-state fMRI global signal amplitude between eyes-open and eyes-closed states to EEG vigilance (50), and the second study documented fMRI BOLD signal fluctuations to eye-closure and invasive electrophysiological recordings in primates (51). Although relevant and buttressing the claims made here, these studies did not specifically address the triune relationship between fMRI DFC, eyelid status, and vigilance behavior documented here.

**Broader Implications of DCS Identification.** A recent meta-analysis of resting-state FC studies found that when using sophisticated fMRI signal analysis methods, epochs containing sleep are present in up to a third of awake studies (5). Because falling asleep modulates FC, proper characterization of awake resting-state FC requires consideration of how frequently such sleep epochs occur. The present work begs the questions: What if, apart from voluntary sleep deprivation, a participant has increased dwell time in the low-arousal state? Would post hoc editing of sleepy epochs using machine-learning techniques be beneficial or would it also remove informative connectivity patterns? Patients with attention-deficit hyperactivity disorder, for example, show increased variance in response times (52) that could be mirrored in increased dwell time in our low-arousal state.

Whereas the present results show an unequivocal link between specific DCS and arousal/vigilance, the high dimensionality of DFC data are such that depending on the behavioral metric used, different states may be uncovered. As such, it is important to point out that although we focused specifically on vigilance, pegging a pattern classifier to other interesting mental states should be feasible, the key challenge being to find a physiological proxy for mental state of interest that can be observed without interrupting the natural flow of thought. A particularly fertile ground to explore would be heterogeneous mind-wandering states (53). Future work could also lend fresh meaning to the metaphor "changing mental gears" when speaking of transitions in mental effort.

## Conclusion

By using SECs as a proxy, we tracked temporal fluctuations in behavioral states without relying on potentially disruptive mental probes. We established a direct association between two patterns of FC fluctuations and arousal.

## Materials and Methods

**Participants, Data Acquisition, and Preprocessing.** Data from 18 participants (9 males; aged 22 ± 2 y) were included in the analyses. All participants provided informed consent in compliance with a protocol approved by the National University of Singapore Institutional Review Board. They were screened for regular sleeping habits and their sleep patterns were monitored 1 wk before the scan (*SI Materials and Methods*). All participants were scanned at 6:00 AM following 1 night of ∼22-h sleep deprivation (Fig. 1, step 1). Each session comprised two 6-min task-free fMRI runs, once before and once after six 10-min AVT runs (*SI Materials and Methods*). An eye-tracking camera (NordicNeuroLab) was used to monitor spontaneous eyelid closures throughout the session. fMRI data were preprocessed following our previously described procedures (54) using the FMRIB Software Library (55) and the AFNI software (56) (*SI Materials and Methods*).

**Identifying SEC-Associated DFC States at Rest.** DFC analyses were performed based on a predefined set of 126 ROIs, which included 114 cortical regions derived from an independent analysis of whole-brain functional organization in a large sample of 1,000 subjects (57) and 12 subcortical structures from the Automated Anatomical Labeling template (58). The 114 cortical regions were further grouped into eight intrinsic connectivity networks: the DMN, control, limbic, visual, somatosensory, temporal-parietal, ventral attention, and DAN (57).

DFC between the 126 ROIs was estimated using a sliding-window approach (11). Specifically, tapered time windows were created by convolving a rectangle (width = 40 s) with a Gaussian window (window $\alpha = 6$ s). The covariance matrices of the windowed fMRI data were estimated from a regularized precision matrix using graphical LASSO methods (59, 60). L1 norm penalties were applied on the precision matrices to promote sparsity and were the group mean of individually optimized L1 penalties based on the log-likelihood of unobserved data, as previously described (11). This was repeated successively along the fMRI time course in steps of 1 repetition time (TR; 2 s), resulting in 156 windowed covariance matrices per 6-min run. We also repeated the analyses using 30-, 70-, and 100-s window lengths to ensure the robustness of our findings.

To derive distinct DCS, a *k*-means clustering algorithm was applied to all windowed covariance matrices (18 subjects × 2 runs × 156 windows per runs = 5,616 windows) using city block distance as the similarity measure. To reduce redundancy between time windows and to reduce computational load, we performed subsampling along the temporal dimension to identify windowed covariance matrices with local maxima in FC variance. This resulted in a subset of 334 windows that were clustered using *k*-means. The optimal number of clusters (*k*) was determined to be nine based on elbow criterion, computed as the ratio of within-cluster to between-cluster distances, after searching a range of *k* from 2 to 10. Clustering was repeated 10 times with random initialization of starting centroid locations. The resulting centroids from the subsamples were then used as the starting point for clustering of all data (5,616 windows) (Fig. 1, step 2). We repeated the same procedure for different numbers of clusters $k = 3$, 5, and 7.

To identify SEC-related DCS, we correlated the probabilities of DCS occurrence with SEC scores using Spearman's rank correlation. The same tapered time window used previously for fMRI data analysis was applied to the time courses of SEC scores to derive SEC ratings per window. These windowed SEC scores were subsequently binned into 8 (1-2-8-9) to estimate the probability of DCS occurrences for each SEC bin (Fig. 1, step 3). The occurrence probability of each DCS at each SEC bin was estimated as the proportion of time each windowed connectivity matrix was assigned to that DCS cluster.

**Deriving High- and Low-Arousal DFC States from Task-Based fMRI and Correlating These with AVT Performance.** The sliding-window analysis and *k*-means clustering performed on task-based fMRI data followed the same steps as task-free fMRI data described above. We regressed out task-related activation from BOLD time courses before sliding-window analysis (*SI Materials and Methods*). We used the FC patterns of high- and low-arousal DCS derived from task-free data as state templates. The DCS obtained from the task condition matched to these state templates were identified based on a pairwise matching method using Pearson's correlation coefficients as the spatial similarity index (Fig. 1, step 4). We also repeated the template matching procedure using city block distances between paired matrices.

Individual differences in AVT performance were correlated with probability of occurrence of the matching task DCS using Spearman's rank correlation coefficient. The proportion of AVT lapses was defined as the ratio between trials of no response or with reaction time greater than 800 ms (2× mean reaction time) to the total number of trials administered (Fig. 1, step 5).

Intrasubject moment-to-moment AVT performance was correlated with the arousal-associated DCS profiles over time. We computed the spatial similarity of the FC pattern of each window to the patterns in high- and low-arousal DCS, respectively. To control the shared information between the two arousal states, partial correlations were used. To characterize the brain–behavior relationship across all AVT trials, including those with no response, we first categorized reaction times of all responded trials into 10 ranks (e.g., the rank of 1 corresponds to the fastest 10% of trials). Trials with no response were assigned the rank of 11. For each participant, the mean rank of all trials within each window was calculated and then correlated with its spatial similarity index to high- and low-arousal states using Pearson's correlation. To test if these brain–behavior relationships were consistent across all subjects, each individual's correlation coefficients were Fisher *Z*-transformed and tested using a one-sample *t* test.

**Replication Analyses Based on Partial Sleep-Deprivation Data.** The partial sleep-deprivation dataset comprised of 17 participants (age = 22.2 ± 1.8, 9 males) was acquired from an independent study (*SI Results*, *Replication Study*). The participant selection criteria and experimental set-up were similar to the main dataset, except for the following: (*i*) subjects were restricted to 5 h of nocturnal sleep on the previous night and underwent scans at 3:00 PM, (*ii*) the two 6-min task-free fMRI scans were performed back-to-back at the beginning, and (*iii*) concurrent EEG data were collected. Both task-free and task-based imaging data were preprocessed and analyzed using the same DFC method as those in the total sleep-deprivation dataset.

**ACKNOWLEDGMENTS.** The study was supported by grants from National Medical Research Council, Singapore (NMRC/STaR/0004/2008 and NMRC/STaR/0015/2013) and the Far East Organization (to M.W.L.C.); Biomedical Research Council, Singapore Grant BMRC 04/1/36/372 (to J.Z.); National Medical Research Council, Singapore Grant CBRG/0088/2015 (to J.Z.); and Duke-National University of Singapore Medical School Signature Research Program, funded by the Ministry of Health, Singapore (to J.Z.).

1. Fox MD, Raichle ME (2007) Spontaneous fluctuations in brain activity observed with functional magnetic resonance imaging. *Nat Rev Neurosci* 8(9):700–711.
2. Sonuga-Barke EJ, Castellanos FX (2007) Spontaneous attentional fluctuations in impaired states and pathological conditions: A neurobiological hypothesis. *Neurosci Biobehav Rev* 31(7):977–986.
3. Handwerker DA, Roopchansingh V, Gonzalez-Castillo J, Bandettini PA (2012) Periodic changes in fMRI connectivity. *Neuroimage* 63(3):1712–1719.
4. Hutchison RM, et al. (2013) Dynamic functional connectivity: Promise, issues, and interpretations. *Neuroimage* 80:360–378.
5. Tagliazucchi E, Laufs H (2014) Decoding wakefulness levels from typical fMRI resting-state data reveals reliable drifts between wakefulness and sleep. *Neuron* 82(3): 695–708.
6. Barttfeld P, et al. (2015) Signature of consciousness in the dynamics of resting-state brain activity. *Proc Natl Acad Sci USA* 112(3):887–892.
7. Hampson M, Driesen NR, Skudlarski P, Gore JC, Constable RT (2006) Brain connectivity related to working memory performance. *J Neurosci* 26(51):13338–13343.
8. Di Martino A, et al. (2009) Relationship between cingulo-insular functional connectivity and autistic traits in neurotypical adults. *Am J Psychiatry* 166(8):891–899.
9. Seeley WW, et al. (2007) Dissociable intrinsic connectivity networks for salience processing and executive control. *J Neurosci* 27(9):2349–2356.
10. Rosenberg MD, et al. (2016) A neuromarker of sustained attention from whole-brain functional connectivity. *Nat Neurosci* 19(1):165–171.
11. Allen EA, et al. (2014) Tracking whole-brain connectivity dynamics in the resting state. *Cereb Cortex* 24(3):663–676.
12. Shirer WR, Ryali S, Rykhlevskaia E, Menon V, Greicius MD (2012) Decoding subject-driven cognitive states with whole-brain connectivity patterns. *Cereb Cortex* 22(1): 158–165.
13. Birn RM, Diamond JB, Smith MA, Bandettini PA (2006) Separating respiratory-variation-related fluctuations from neuronal-activity-related fluctuations in fMRI. *Neuroimage* 31(4):1536–1548.
14. Chang C, Glover GH (2009) Effects of model-based physiological noise correction on default mode network anti-correlations and correlations. *Neuroimage* 47(4): 1448–1459.
15. Smallwood J, et al. (2013) Escaping the here and now: Evidence for a role of the default mode network in perceptually decoupled thought. *Neuroimage* 69:120–125.
16. Mason MF, et al. (2007) Wandering minds: The default network and stimulus-independent thought. *Science* 315(5810):393–395.
17. Andrews-Hanna JR (2012) The brain's default network and its adaptive role in internal mentation. *Neuroscientist* 18(3):251–270.
18. Calhoun VD, Miller R, Pearlson G, Adalı T (2014) The chronnectome: Time-varying connectivity networks as the next frontier in fMRI data discovery. *Neuron* 84(2): 262–274.
19. Chang C, Liu Z, Chen MC, Liu X, Duyn JH (2013) EEG correlates of time-varying BOLD functional connectivity. *Neuroimage* 72:227–236.
20. de Pasquale F, et al. (2010) Temporal dynamics of spontaneous MEG activity in brain networks. *Proc Natl Acad Sci USA* 107(13):6040–6045.
21. Chang C, et al. (2013) Association between heart rate variability and fluctuations in resting-state functional connectivity. *Neuroimage* 68:93–104.
22. Smallwood J, et al. (2004) Subjective experience and the attentional lapse: Task engagement and disengagement during sustained attention. *Conscious Cogn* 13(4): 657–690.
23. Ong JL, Asplund CL, Chia TT, Chee MW (2013) Now you hear me, now you don't: Eyelid closures as an indicator of auditory task disengagement. *Sleep* 36(12): 1867–1874.
24. Dinges DF, Mallis MM, Maislin G, Powell JW (1998) *Evaluation of Techniques for Ocular Measurement as an Index of Fatigue and the Basis for Alertness Management, NHTSA report no. DOT HS 808 762* (National Highway Traffic Safety Administration, Washington, DC).
25. Johns MW, Tucker A, Chapman R, Crowley K, Michael N (2007) Monitoring eye and eyelid movements by infrared reflectance oculography to measure drowsiness in drivers. *Somnologie (Berl)* 11(4):234–242.
26. Ong JL, et al. (2015) Co-activated yet disconnected—Neural correlates of eye closures when trying to stay awake. *Neuroimage* 118:553–562.
27. Sämann PG, et al. (2010) Increased sleep pressure reduces resting state functional connectivity. *MAGMA* 23(5-6):375–389.
28. De Havas JA, Parimal S, Soon CS, Chee MW (2012) Sleep deprivation reduces default mode network connectivity and anti-correlation during rest and task performance. *Neuroimage* 59(2):1745–1751.
29. Yeo BT, Tandi J, Chee MW (2015) Functional connectivity during rested wakefulness predicts vulnerability to sleep deprivation. *Neuroimage* 111:147–158.
30. Spoormaker VI, et al. (2010) Development of a large-scale functional brain network during human non-rapid eye movement sleep. *J Neurosci* 30(34):11379–11387.
31. Doran SM, Van Dongen HP, Dinges DF (2001) Sustained attention performance during sleep deprivation: Evidence of state instability. *Arch Ital Biol* 139(3):253–267.
32. Leonardi N, Van De Ville D (2015) On spurious and real fluctuations of dynamic functional connectivity during rest. *Neuroimage* 104:430–436.
33. Christoff K, Gordon AM, Smallwood J, Smith R, Schooler JW (2009) Experience sampling during fMRI reveals default network and executive system contributions to mind wandering. *Proc Natl Acad Sci USA* 106(21):8719–8724.
34. Richiardi J, Eryilmaz H, Schwartz S, Vuilleumier P, Van De Ville D (2011) Decoding brain states from fMRI connectivity graphs. *Neuroimage* 56(2):616–626.
35. Fox MD, et al. (2005) The human brain is intrinsically organized into dynamic, anti-correlated functional networks. *Proc Natl Acad Sci USA* 102(27):9673–9678.
36. Strijkstra AM, Beersma DG, Drayer B, Halbesma N, Daan S (2003) Subjective sleepiness correlates negatively with global alpha (8–12 Hz) and positively with central frontal theta (4–8 Hz) frequencies in the human resting awake electroencephalogram. *Neurosci Lett* 340(1):17–20.
37. Klimesch W (1999) EEG alpha and theta oscillations reflect cognitive and memory performance: A review and analysis. *Brain Res Brain Res Rev* 29(2-3):169–195.
38. Makeig S, Jung TP (1996) Tonic, phasic, and transient EEG correlates of auditory awareness in drowsiness. *Brain Res Cogn Brain Res* 4(1):15–25.
39. Tijerina LGM, Stoltzfus D, Johnston S, Goodman MJ, Wierwille WW (1998) *A Preliminary Assessment of Algorithms for Drowsy and Inattentive Driver Detection on the Road* (National Highway Traffic Safety Administration, Washington, DC).
40. Portas CM, et al. (2000) Auditory processing across the sleep-wake cycle: Simultaneous EEG and fMRI monitoring in humans. *Neuron* 28(3):991–999.
41. Massimini M, et al. (2005) Breakdown of cortical effective connectivity during sleep. *Science* 309(5744):2228–2232.
42. Larson-Prior LJ, et al. (2009) Cortical network functional connectivity in the descent to sleep. *Proc Natl Acad Sci USA* 106(11):4489–4494.
43. Horovitz SG, et al. (2009) Decoupling of the brain's default mode network during deep sleep. *Proc Natl Acad Sci USA* 106(27):11376–11381.
44. Van Dijk KR, et al. (2010) Intrinsic functional connectivity as a tool for human connectomics: Theory, properties, and optimization. *J Neurophysiol* 103(1):297–321.
45. Poudel GR, Innes CR, Bones PJ, Watts R, Jones RD (2014) Losing the struggle to stay awake: Divergent thalamic and cortical activity during microsleeps. *Hum Brain Mapp* 35(1):257–269.
46. Tononi G, Massimini M (2008) Why does consciousness fade in early sleep? *Ann N Y Acad Sci* 1129:330–334.
47. Sämann PG, et al. (2011) Development of the brain's default mode network from wakefulness to slow wave sleep. *Cereb Cortex* 21(9):2082–2093.
48. Boveroux P, et al. (2010) Breakdown of within- and between-network resting state functional magnetic resonance imaging connectivity during propofol-induced loss of consciousness. *Anesthesiology* 113(5):1038–1053.
49. Hannawi Y, Lindquist MA, Caffo BS, Sair HI, Stevens RD (2015) Resting brain activity in disorders of consciousness: A systematic review and meta-analysis. *Neurology* 84(12): 1272–1280.
50. Wong CW, DeYoung PN, Liu TT (2016) Differences in the resting-state fMRI global signal amplitude between the eyes open and eyes closed states are related to changes in EEG vigilance. *Neuroimage* 124(Pt A):24–31.
51. Chang C, et al. (2016) Tracking brain arousal fluctuations with fMRI. *Proc Natl Acad Sci USA* 113(16):4518–4523.
52. Castellanos FX, et al. (2005) Varieties of attention-deficit/hyperactivity disorder-related intra-individual variability. *Biol Psychiatry* 57(11):1416–1423.
53. Fox KC, Spreng RN, Ellamil M, Andrews-Hanna JR, Christoff K (2015) The wandering brain: Meta-analysis of functional neuroimaging studies of mind-wandering and related spontaneous thought processes. *Neuroimage* 111:611–621.
54. Ng KK, Lo JC, Lim JK, Chee MW, Zhou J (2016) Reduced functional segregation between the default mode network and the executive control network in healthy older adults: A longitudinal study. *Neuroimage* 133:321–330.
55. Jenkinson M, Beckmann CF, Behrens TE, Woolrich MW, Smith SM (2012) FSL. *Neuroimage* 62(2):782–790.
56. Cox RW (1996) AFNI: Software for analysis and visualization of functional magnetic resonance neuroimages. *Comput Biomed Res* 29(3):162–173.
57. Yeo BT, et al. (2011) The organization of the human cerebral cortex estimated by intrinsic functional connectivity. *J Neurophysiol* 106(3):1125–1165.
58. Tzourio-Mazoyer N, et al. (2002) Automated anatomical labeling of activations in SPM using a macroscopic anatomical parcellation of the MNI MRI single-subject brain. *Neuroimage* 15(1):273–289.
59. Smith SM, et al. (2011) Network modelling methods for FMRI. *Neuroimage* 54(2): 875–891.
60. Friedman J, Hastie T, Tibshirani R (2008) Sparse inverse covariance estimation with the graphical lasso. *Biostatistics* 9(3):432–441.
61. Horne JA, Ostberg O (1976) A self-assessment questionnaire to determine morningness-eveningness in human circadian rhythms. *Int J Chronobiol* 4(2):97–110.
62. Ong JL, Lo JC, Gooley JJ, Chee MW (2016) EEG across multiple nights of sleep restriction and recovery in adolescents: The Need for Sleep study. *Sleep* 39(6): 1233–1240.
63. Zuo XN, et al. (2010) Reliable intrinsic connectivity networks: Test-retest evaluation using ICA and dual regression approach. *Neuroimage* 49(3):2163–2177.
64. Greve DN, Fischl B (2009) Accurate and robust brain image alignment using boundary-based registration. *Neuroimage* 48(1):63–72.
65. Geerligs L, Renken RJ, Saliasi E, Maurits NM, Lorist MM (2015) A brain-wide study of age-related changes in functional connectivity. *Cereb Cortex* 25(7):1987–1999.
66. Fukunaga M, et al. (2006) Large-amplitude, spatially correlated fluctuations in BOLD fMRI signals during extended rest and early sleep stages. *Magn Reson Imaging* 24(8): 979–992.